

A Dimeric Thymol Derivative from *Arnica sachalinensis*

Claus M. Passreiter^{1*}, Günter Willuhn¹, Horst Weber² and Klaus-Jürgen Schleifer²

¹ Institut für Pharmazeutische Biologie,
² Institut für Pharmazeutische Chemie,
Heinrich-Heine-Universität Düsseldorf,
Universitätsstrasse 1,
D-40225 Düsseldorf, Germany

Received 12 November 1998; accepted 22 January 1999

Abstract: A novel, unusual terpenoid compound was found as one of the main constituents in *Arnica sachalinensis* (Asteraceae). Its structure was established by NMR spectroscopic studies including COSY, HMQC, HMBC, and DEPT-135 experiments as a dimeric thymol derivative with a new spiro[benzofuran-3(2*H*),2'-pyrano[2,3-*b*]benzofuran] ring system. The stereochemistry and a possible biosynthesis of this compound are discussed and its antifeedant activity was tested against 5th instar larvae of *Spodoptera litura*, using leaf disk bioassays. © 1999 Elsevier Science Ltd. All rights reserved.

Keywords: *Arnica sachalinensis*, Asteraceae, terpenoids, thymol derivatives, antifeedant activity, *Spodoptera litura*, molecular modeling.

Thymol derivatives, widely distributed within the Asteraceae, are useful chemical features for taxonomic treatments on tribal and subtribal level inside this large family.¹ Recently, we reported the identification of several compounds from this group, including 10-acyloxy derivatives of 8,9-dehydrothymol and 8,9-epoxythymol, as well as 8-hydroxy-9-isobutyryloxythymol and 9-chloro-8,9-dehydrothymol from the flowerheads of the northeast Asian endemic *A. sachalinensis* (Regl.) A. Gray.^{2,3} Moreover, 10-acetoxy-8,9-epoxythymolisobutyrate has been identified as contact allergen.⁴ We now report the isolation and structure elucidation of a new dimeric thymol derivative **1** containing the new tetrahydro-spiro[benzofuran-3(2*H*),2'-pyrano[2,3-*b*]benzofuran] ring system as one of the main constituents of *A. sachalinensis* (Regl.) A. Gray.

Separation of the petroleum ether extract of the flowerheads by column chromatography on silica gel (see Experimental) yielded two fractions containing compound **1**. Further purification using alumina gave 138 mg white, microcrystalline **1**. In accordance with most of the other thymol ester derivatives isolated from *A. sachalinensis*^{2,3}, **1** was detectable in TLC as dark spot in UV light ($\lambda=254$ nm) and by the violet color of its reaction products obtained after treatment with anise aldehyde-H₂SO₄ and heating.

The fragmentation pattern of **1** in the mass spectrum (EI) was in parts similar to those of other previously isolated compounds.^{2,3} Its molecular ion registered at *m/z* 340, and confirmed by FAB-MS ([M+H]⁺ = 341), was consistent with the formula C₂₀H₂₀O₅. Further characteristic ions were found at *m/z* 322 [M - H₂O]⁺, 311

$[M - CHO]^+$ and 293 $[M - (H_2O + CHO)]^+$, due to the loss of H_2O and an aldehyde function, respectively. The base ion was detected at m/z 135, also found for thymol and some of its derivatives.^{2,5}

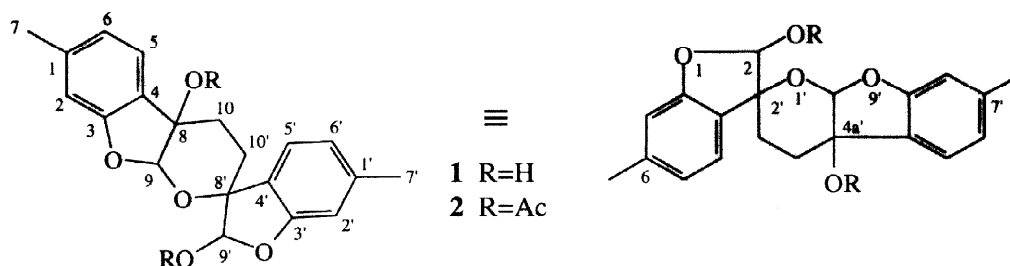


Fig. 1: Structures of **1** and **2** numbered according to thymol (left formula) and to CA ring index nomenclature (3',4',4a',9a'-Tetrahydro-6,7'-dimethyl-spiro[benzofuran-3(2*H*),2'-pyrano[2,3-*b*]benzofuran]-2,4a'-diol (**1**), right formula). Due to the proposed biochemical pathway (see Fig. 3) the thymol-derived numbering was used among the whole manuscript.

The structure of **1** was unambiguously established by ^{13}C and 1H NMR spectroscopic studies, including 2D-HMQC, 2D-HMBC, 2D-COSY and DEPT-135 experiments. The ^{13}C NMR spectra showed the signals for ten pairs of carbons, indicating the presence of two similar parts in the structure of **1**. Seven pairs could be assigned to two triple substituted benzene rings (C-1 to C-6 and C-1' to C-6' respectively, see Table 1), each bearing a methyl group attached to C-1, which thus represented the benzene moieties of two thymol substructures.^{2,3} The corresponding protons (see Table 2) could easily be assigned using the 2D-HMQC spectrum. The remaining six carbons were identified as one pair of methylene (δ 31.13 and 23.57 ppm, C-10 and C-10', respectively), methine (δ 111.5 and 108.09 ppm, C-9 and C-9', respectively), and quaternary carbons (δ 77.24 and 83.63 ppm, C-8 and C-8', respectively), the latter four were attached to oxygen, deducible from their shift values. Both methine carbons were found at shift values characteristic for acetalic or hemi-acetalic groups, which were built from two underlying aldehydes after reaction with one or two alcoholic or phenolic groups, respectively. In agreement with these findings, the highfield region of the 1H NMR spectra displayed the signals for a $-CH_2-CH_2-$ structure element, whose couplings clearly indicated that both methylene groups are not attached to any further hydrogenated carbon (see Table 2).

The proton signals corresponding to the anomeric carbons of the acetalic and hemi-acetalic functions, were found as signal for one proton each at δ 5.71 (s), 5.89 (d) and 6.24 (d) ppm. After addition of D_2O the doublet at δ 5.89 ppm was simplified to a singlet and the doublet at δ 6.24 ppm decreased. These two signals therefore belong to a hemi-acetalic group, consisting of the acetalic H-9' (δ 5.89 ppm) and the corresponding OH at δ 6.24 ppm.

Thus the hemi-acetal was built from an aldehyde (C-9') attached to C-8' and the phenolic hydroxy group at C-3'. The remaining singlet at δ 5.71 ppm, due to the second acetalic proton (H-9), indicates a full acetal built up from the aldehyde at C-8 with the C-3 hydroxy group and the tertiary alcohol at C-8'. One further singlet, which equally disappeared after addition of D₂O, was displayed at δ 4.94 ppm in the ¹H NMR, thus belonging to a second hydroxy function attached to the quaternary C-8.

All assignments of carbon and proton signals (see Tables 1 and 2) were made by interpretation of the 2D-HMQC and 2D-HMBC spectra, which also allowed the assignment of all quaternary carbons.

Table 1: ¹³C NMR data of compound **1** and **2** (δ (ppm), 125 MHz, acetone-d₆, TMS)

Position	1	DEPT	2
1	141.12	C	141.87
2	111.97	CH	111.42
3	159.97	C	159.36
4	129.57	C	123.71
5	122.54	CH	124.03
6	125.00	CH	123.25
7	21.85	CH ₃	21.08
8	77.24	C	85.11
9	111.50	CH	107.62
10	31.13	CH ₂	27.27
1'	141.75	C	141.87
2'	112.10	CH	110.67
3'	160.78	C	159.66
4'	128.66	C	127.06
5'	123.18	CH	125.65
6'	124.55	CH	122.80
7'	21.83	CH ₃	21.12
8'	83.63	C	82.27
9'	108.09	CH	103.27
10'	23.57	CH ₂	22.67
Ac at C-8	-	CH ₃	21.05
	-	C	169.63
Ac at C-9'	-	CH ₃	20.00
	-	C	168.81

The presence of two free OH groups was additionally confirmed by acetylation of **1**. The corresponding diacetate **2** was equally identified by spectroscopic methods (see Tables 1 and 2). The acetylation of the tertiary alcohol at C-8 was deducible from a downfield shift of C-8 ($\Delta\delta$ = 7.9 ppm) and corresponding upfield shifts for the three carbons C-4 ($\Delta\delta$ = 5.9 ppm), C-9 ($\Delta\delta$ = 3.9 ppm) and C-10 ($\Delta\delta$ = 3.9 ppm) directly attached to C-8. The second acetylation at C-9' was seen by an expected downfield shift of H-9' in the ¹H NMR. The

corresponding carbon (C-9') was shifted upfield by 4.8 ppm due to its anomeric character. Such shift differences were also found for gluco- and galactopyranoside derivatives acetylated at the anomeric C-1.⁶

There was no evidence for the stereochemistry of **1** from its NMR data, but all previously described hydrated pyrano[2,3-*b*]benzofuran ring systems were found to be cis-annelated.⁷⁻⁹ It can therefore be assumed that **1** contains a ring system with the same type of combination, although direct proof is missing in **1**, caused by the replacement of H-8 by a hydroxy group. The configuration at both stereogenic centers (C-8' and C-9') could not be clarified. Analysis of the couplings of the methylene protons (Table 2) showed that the pyran ring in both epimers could either occur in a chair or boat conformation.

Table 2: ¹H NMR data of **1** and **2** (δ (ppm), 500 MHz, acetone-d₆, TMS)

Proton	1	2
H-2	6.63 s	6.74 s (br.)
H-5	7.24 d	7.49 d
H-6	6.79 d	6.87d (br.)
H-7	2.33 s	2.32 s
H-9	5.71 s	6.05 s
H-10a	2.33 m*	2.62 ddd*
H-10b	2.18 ddd*	2.13 dd (br.)*
H-2'	6.64 d	6.65 s (br.)
H-5'	7.39 d	7.38 d
H-6'	6.77 d	6.81 d (br.)
H-7'	2.33 s	2.31 s
H-9'	5.89 d	6.66 s
H-10'a	2.05 m†	2.10 m†
H-10'b	1.93 ddd†	1.68 ddd†
OH at C-8	4.94 s	-
OH at C-9'	6.24 d	-
Ac at C-8	-	2.02 s
Ac at C-9'	-	1.88 s

*, † assignment interchangeable

J (Hz): **1**: 2,6: < 1; 2',6': < 1; 5,6: 7.9; 5',6': 7.9; 10a,10b: 13.3; 10a,10'a: 3.2; 10a,10'b: 11.9; 10b,10'a: 7.0; 10b, 10'b: 3.0; 10'a, 10'b: 14.8; 9',OH: 10.5. **2**: 2,6: 1.5; 2',6': 1.5; 5,6: 7.9; 5',6': 7.7; 10a,10b: 15.1; 10a,10'a: 3.8; 10a,10'b: 11.9; 10b,10'a: 4.4; 10b, 10'b: 5.7; 10'a, 10'b: 14.5.

In order to test the possibility of an energetic differentiation between the chair and boat form a molecular modeling study was performed. Generation of all stereoisomers of **1** was simplified considering the proposed cis-annelated configuration. Therefore the maximum number of 16 stereoisomers resulting from four asymmetric carbon atoms (2⁴) is reduced to 8 diastereomers. Since they represent four enantiomeric pairs (e.g. (8*S*,8'*R*,9*R*,9'*R*)-**1** related to (8*R*,8'*S*,9*S*,9'*S*)-**1**) only four different structures had to be taken into account. To

gain some ideas about their structural flexibility and to yield energetically favorable conformers, high temperature molecular dynamics simulations (mds) followed by molecular mechanics minimizations were carried out. For each stereoisomer two different chair as well as two boat conformers were found and subsequently geometry-optimized applying quantum chemical AM1 computations.

Surprisingly, not depending on the chosen configuration, a slightly distorted boat conformation of the pyrano[2,3-*b*]benzofuran ring system seems to be more favorable (ΔG : 0.49–7.45 kcal/mol) in relation to the chair form (see Table 3).

Table 3: Comparison of potential energies [kcal/mol] derived from ab initio calculations (RHF 6-311G**)

Configuration	ΔG (boat vs. chair)
(8 <i>S</i> ,8' <i>S</i> ,9 <i>R</i> ,9' <i>S</i>)-1	- 7.45
(8 <i>S</i> ,8' <i>S</i> ,9 <i>R</i> ,9' <i>R</i>)-1	- 7.04
(8 <i>S</i> ,8' <i>R</i> ,9 <i>R</i> ,9' <i>R</i>)-1	- 4.99
(8 <i>S</i> ,8' <i>R</i> ,9 <i>R</i> ,9' <i>S</i>)-1	- 0.49

This is supported by the observation that in two cases ((8*S*,8'*S*,9*R*,9'*S*)-1 and (8*S*,8'*S*,9*R*,9'*R*)-1) the chair conformations derived from mds were converted into the boat forms in course of the semiempiric optimization. A closer examination of the chair conformers explains this behavior, since the pyrano[2,3-*b*]benzofuran linking prevents an optimum adjustment of the chair form leading to very flat chairs with an almost half-chair character.

Even though these results must be interpreted very carefully in regard to the NMR results, especially in light of the lacking solvent during molecular modeling investigations, the calculated energy differences up to more than 7 kcal/mol and the observed unusual transition from the chair to the boat form in course of the semiempiric minimizations give rise to the suspicion, that in the special case considered here, the boat conformation seems to be more likely (see Fig. 2).

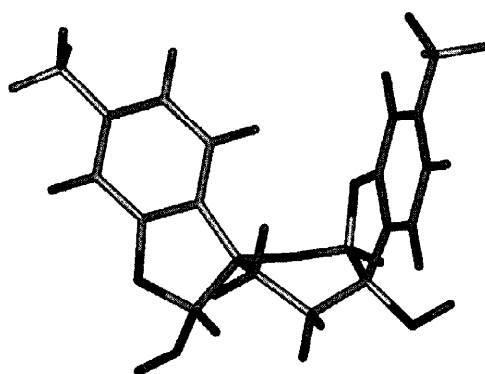


Fig. 2: Energetically favorable boat conformation of the pyran ring derived from molecular modeling investigations (e.g. (8*S*,8'*S*,9*R*,9'*S*)-1).

Independent to the configuration at the anomeric C-9', the only difference between both C-8 epimers has to be seen in the position of the hydroxyl groups, either on the same or different sides of the pyran moiety. Definite proof of the stereochemistry of **1** could therefore only been made by X-ray analysis with appropriate crystals, which have not been received yet.

The biosynthesis of **1** is speculative (see Fig. 3), but it is unlikely that the dimerization occurs via a 8-hydroxy-9-oxo-thymol precursor (way A), because both 10-methyl groups are whatsoever not activated for an oxidative combination. A much better explanation for the formation of the pyran ring is the well known easy hetero-*Diels-Alder* cycloaddition of a corresponding acrolein (way B)^{10,11}, especially because 10-acyloxy-8,9-dehydrothymol derivatives **3**, which are possible precursors for **1** were previously found in *A. sachalinensis*.³

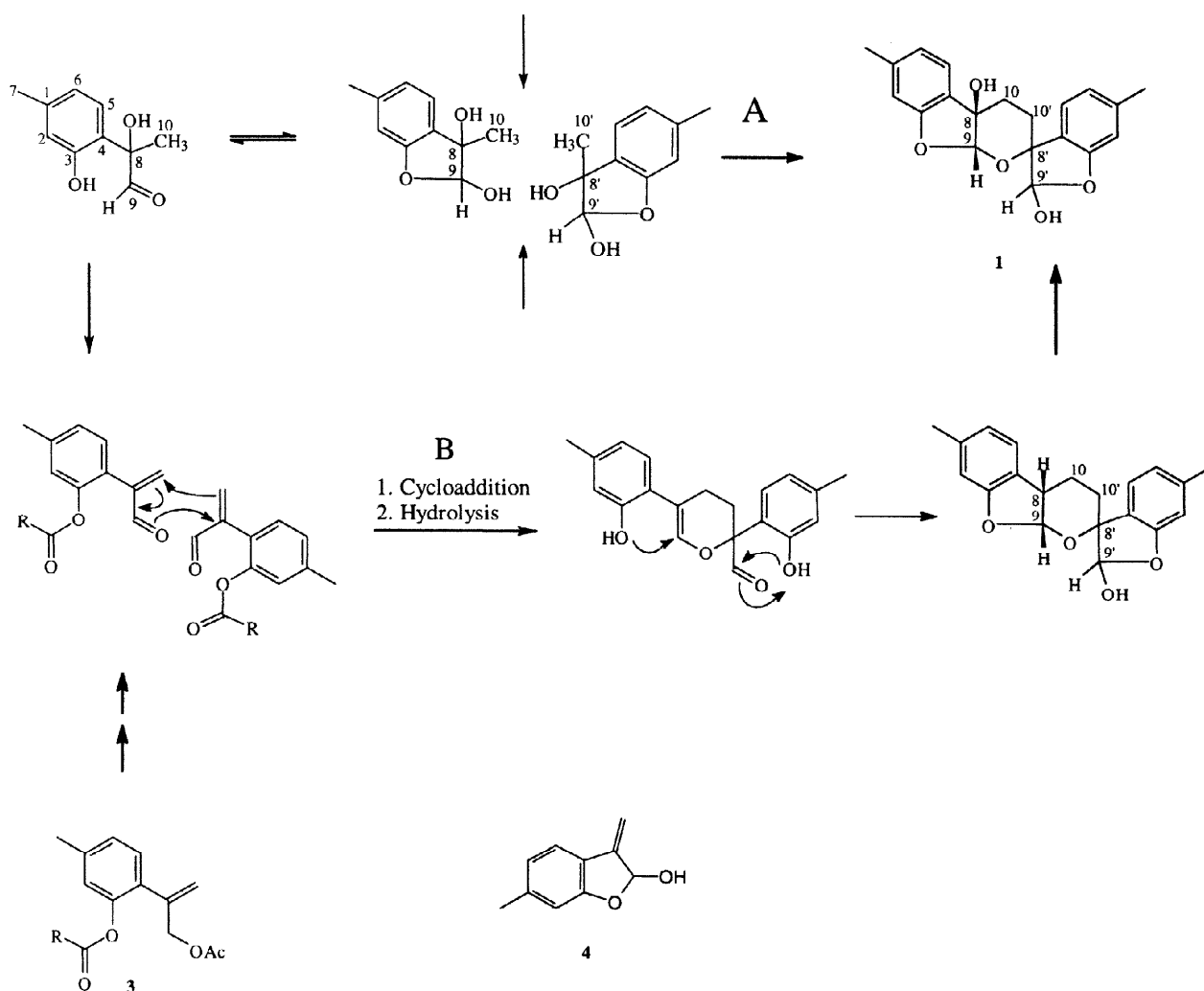


Fig. 3: Proposed biochemical pathway for the biosynthesis of **1**

This is further evident from the occurrence of the cyclic semiacetalic compound **4**, identified in various Asteraceae^{12–14}, which is proofing the existence of such acroleins. The intermediately built dihydropyran-2-carbaldehyde is after hydrolysis predestined for a two-fold addition of the phenolic OH groups, which forms both furan rings. As final step in the biosynthesis of **1** an oxidation at the benzylic C-8 of the pyrano[2,3-*b*]benzofuran moiety has to take place, which should biochemically be possible, especially because other 8-hydroxy derivatives have been found in this plant.²

As **1** is containing two benzofuran moieties and other benzofurans have been found to be active against insects^{15,16}, we have tested the antifeedant activity of **1** in a no-choice leaf disc bioassay, using 5th instar larvae of *Spodoptera litura* (Noctuidae).¹⁷ To evaluate the feeding deterrence, we tested **1** at two concentrations (35 and 70 µg per 1.5 cm²) previously found to be suitable. Based on Anova and Duncan's test, no significant difference was observed between **1** and the control using 35 µg. Applying 70 µg per disk the antifeedant effect of **1** (25.7 % ± 3.9) is not significantly differing from the effect of 10-acetoxy-8,9-epoxy-thymolisobutyrate (38.4 % ± 14.4).¹⁷

Experimental

Plant material: *Arnica sachalinensis* (Regl.) A. Gray was grown from seeds, provided by the Botanical garden of the Academy of Sciences, Moscow, Russia, and cultivated on proving fields of the Botanical Garden of the Heinrich-Heine-Universität Düsseldorf. Vouchers are on deposit at the Herbarium of the Institut für Pharmazeutische Biologie, Heinrich-Heine-Universität Düsseldorf.

Extraction and Isolation: Dried and powdered flowerheads (4.37 kg) were extracted with petroleum ether (40–60°) in a Soxhlet apparatus. The resulting dried extract was dissolved in petroleum ether (10 % g/V) and extracted 8 times with aqueous ethanol (60 %). After evaporation of the ethanol, the resulting aqueous phase was extracted another 8 times with Et₂O. The Et₂O extract (50.7 g = 1.16 % of the dry weight) was first separated by CC on silica gel 60 (Merck) with mixtures of petroleum ether/Et₂O, yielding 3.5 g of a fraction with crude yellow crystalline compound **1**. Further CC of an aliquot (280 mg) on alumina (Woelm, 250 g, activity II) with petroleum ether-benzene-CHCl₃-MeOH (5:4:1:2) gave 138 mg white, microcrystalline compound **1**.

Gas chromatography: GC F 22 (Perkin Elmer), column OV-01 (Macherey&Nagel, Germany), 25m x 0.25 mm. Temp. prog. 120° to 250° at 10°min⁻¹; MS: EI (70 eV) on Varian MAT CH7A; FAB-MS: mass spectrometer MAT 900 (Finnigan MAT, Bremen, Germany).

Nuclear Magnetic Resonance: Bruker AMX 500 or ARX 500, 500 MHz (^1H NMR) and 125 MHz (^{13}C NMR) in acetone- d_6 or Bruker WH 360 (^1H NMR) in CDCl_3 , TMS as internal standard.

Optical rotation: Specific rotation was measured on a Perkin Elmer 341 LC Polarimeter at 20 °C.

Compound 1:

Mp 186 °C; $[\alpha]_{\text{D}}^{20} = 0$; UV (MeOH): λ_{max} : 283 nm, 289 sh (ϵ 7114); IR (ν cm^{-1} , KBr): 3420 and 3335 (OH), 3020, 1615, 1595 and 1505 (benzene moieties), 2680 and 1430 (CH_3) 1150-1050 (C-O), 810 (1,3,5-substituted benzene moiety); TLC (n-pentane-Et $_2$ O 8:17, silica gel 60 F $_{254}$ (Merck)): R_f : 0.41; ^1H and ^{13}C NMR (see Tables 1 and 2); MS: EI, 70 eV, m/z (rel. Int.): 340 $[\text{M}]^+$ (2), 322 $[\text{M}-\text{H}_2\text{O}]^+$ (1), 311 $[\text{M}-\text{CHO}]^+$ (34), 293 $[\text{M}-\text{H}_2\text{O}-\text{CHO}]^+$ (4), 283 (5), 265 (2), 203 (8), 175 (15), 163 (6), 162 (9), 161 (8), 159 (4), 158 (4), 151 (3), 148 (2), 147 (4), 145 (4), 136 (10), 135 (100), 134 (4), 133 (6), 132 (3), 131 (8), 121 (2), 119 (3), 116 (2), 107 (2), 105 (5), 91 (7), 79 (2), 77 (4), 55 (4), 51 (1), 43 (4). FAB, m/z (rel. Int.): 341 $[\text{M}+\text{H}]^+$ (38), 135 (100).

Acetylation of 1: 1.0 ml of a solution of **1** (20 mg) in Ac $_2$ O/pyridine (1:1) were stirred at room temperature for 48 h. After evaporation of the solvent in vacuo at room temperature **2** was obtained by recrystallization from acetone.

Compound 2:

Mp 199-202 °C; $[\alpha]_{\text{D}}^{20} = 0$; IR (ν cm^{-1} , KBr): 3035, 1620, 1595 and 1495 (benzene moieties), 2880 and 1430 (CH_3) 1755 (ester), 1240 and 1215 (acetate) 1125-1150 (C-O), 810 (1,3,5-substituted benzene moiety); GC-MS, 70 eV m/z (rel. Int.): 424 $[\text{M}]^+$ (18), 364 $[\text{M}-\text{AcOH}]^+$ (12), 322 $[\text{M}-\text{AcOH}-\text{CH}_2=\text{C}=\text{O}]^+$ (7), 321 $[\text{M}-\text{AcOH}-\text{Ac}]^+$ (6), 304 $[\text{M}-(2*\text{AcOH})]^+$ (82), 293 $[\text{M}-\text{AcOH}-\text{CH}_2=\text{C}=\text{O}-\text{CHO}]^+$ (24), 276 (14), 275 $[\text{M}-(2*\text{AcOH})-\text{CHO}]^+$ (12), 217 (40), 204 (30), 175 (99), 163 (39), 162 (74), 158 (70), 135 (100) 115 (17), 105 (21), 91 (19), 77 (31), 51 (13), 43 (97); ^1H NMR (360 MHz, CDCl_3 , TMS): 6.72 s (br.) (H-2), 7.43 d (H-5), 6.81 d (br.) (H-6), 2.35 s (H-7), 5.72 s (H-9), 2.77 m (H-10a), 2.56 ddd (H-10b), 6.78 s (br.) (H-2'), 7.40 d (H-5'), 6.87 d (br.) (H-6'), 2.34 s (H-7'), 6.08 s (H-9'), 2.12 m (H-10'a), 1.71 ddd (H-10'b), 2.07 s (Ac at C-8), 1.93 s (Ac at C-9'). See table 2 for data in acetone- d_6 and table 1 for ^{13}C NMR data. TLC (n-pentane-Et $_2$ O 8:17): 0.6; GC: R_t (min.): 16.7.

Bioassay: Assays were performed as described previously.¹⁷ Images of the leaf discs were produced using a Hewlett-Packard Scanjet HP-6c and saved as electronic files.¹⁸ These images were analyzed using the

public domain NIH Image program Scion Image (available from the National Institute of Health at <http://rsb.info.nih.gov/nih-image/>) to get the consumed area. The feeding deterrence was calculated as % deterrence = $100 - ((\text{consumed area treated disc} \times 100) / \text{consumed area control})$.

Molecular modeling: All molecular dynamics simulations (mds) were carried out on Silicon Graphics workstations applying the software package Insight/Discover[®] (Molecular Simulations Inc.). In order to overcome the restricted flexibility of the spiro-linked compounds a temperature of 1500 K was chosen. Subsequent to an initialization period of 90 ps, a simulated annealing protocol was repeated 30 times cooling the system down to 0 K during 30 ps. The resulting 30 geometry-optimized conformers were clustered and similar derivatives (in relation to the pyran conformation) were assigned into one family yielding two energetically favorable chair and boat families. From each family the lowest energy conformer was fully geometry-optimized employing the semiempiric AM1 method of SPARTAN (Wavefunction Inc.). Potential energies of the AM1-optimized structures were determined by quantum chemical (RHF) ab initio calculations using the 6-311G** basis set.

Acknowledgements

We are grateful to Prof. Dr. H.-D. Höltje, Institut für Pharmazeutische Chemie, Heinrich-Heine-Universität Düsseldorf, for providing all hard- and software for the molecular modeling investigations. We thank Dr. D. Wendisch, ZF-DZA Strukturchemie, Bayer AG, Leverkusen and Dr. W. Peters and his coworkers, Institut für Anorganische Chemie und Strukturchemie, Heinrich-Heine-Universität Düsseldorf, for recording the NMR spectra and to Mrs Heike Fürtges, Institut für Pharmazeutische Biologie, Heinrich-Heine-Universität Düsseldorf, for technical assistance.

References

1. Bohm, B.A. in *The Biology and the Chemistry of the Compositae* (Heywood, J.B.; Harborne, B.L.; Turner, B.L., eds.) **1977**, pp. 746, Academic Press, London.
2. Willuhn, G.; Junior, I.; Wendisch, D. *Planta Med.* **1986**, 349.
3. Passreiter, C.M.; Willuhn, G.; Matthiesen, U. *Phytochemistry* **1998**, 49, 777.
4. Paßreiter, C.M.; Florack, M.; Willuhn, G.; Goerz, G. *Dermatosen Beruf Umwelt* **1988**, 36, 79.
5. Sydow, E. von *Acta Chem. Scand.* **1963**, 17, 2504.
6. Lee, E.; O'Callaghan, J.; O'Reilly, J. P. *Carbohydr. Res.* **1982**, 105, 266.
7. Roy, R.S.; Mandal, P. K. *Tetrahedron* **1996**, 52, 12495.

8. De Meesmaker, A.; Hoffmann, P.; Ernst, B. *Tetrahedron Lett.* **1988**, 29, 6585.
9. Kuser, P.; Frauenfelder, E.F.; Eugster, C.H. *Helv. Chim. Acta* **1971**, 54, 969.
10. Alder, K.; Rüden, E. *Ber. Dtsch. Chem. Ges.* **1941**, 74, 920.
11. Alder, K.; Offermanns, H.; Rüden, E. *Ber. Dtsch. Chem. Ges.* **1941**, 74, 926.
12. Bohlmann, F.; Schulz, J.; Bühmann, U. *Tetrahedron Lett.* **1969**, 53, 4703.
13. Gommers, F.J. *Nematologica* **1972**, 18, 458.
14. Bohlmann, F.; Natu, A.A.; Kerr, K. *Phytochemistry* **1979**, 18, 489.
15. Ishibashi, F.; Satasook, C.; Isman, M.B.; Towers, G.H.N. *Phytochemistry* **1993**, 32, 307.
16. Proksch, P.; Proksch, M.; Towers, G.H.N.; Rodriguez, E. *J. Nat. Prod.* **1983**, 46, 331.
17. Passreiter, C.M.; Isman, M.B. *Biochem. Syst. Ecol.* **1997**, 25, 371.
18. Bomford, M.K.; Isman, M.B. *Entomol. Exp. Appl.* **1996**, 81, 307.